

Lattice QCD calculation of K^+K^- scattering length

Ziwen Fu

Key Laboratory for Radiation Physics and Technology of Education Ministry; Institute of Nuclear Science and Technology, College of Physical Science and Technology, Sichuan University, Chengdu 610064, People's Republic of China.

(Dated: October 19, 2012)

We deliver ab initio calculation of s -wave K^+K^- scattering length ($a_0^{K^+K^-}$) by Lüscher's formula. In the "Asqtad" improved staggered dynamical fermion formulation, we measure K^+K^- four-point correlation function by moving wall sources without gauge fixing, and find $a_0^{K^+K^-} = 0.456 \pm 0.272$ fm, which is in reasonable agreement with tree-level prediction and comparable with experimental result. An essential ingredient in our calculation is to explicitly include the disconnected diagram.

PACS numbers: 12.38.Gc

K^+K^- interactions are still very poorly understood. Our basic motivation for investigating K^+K^- scattering via lattice QCD is preliminarily discussed in Ref. [1], as an attempt to unveil the mysterious nature of the scalar resonances $a_0(980)/f_0(980)$, as well as the $\phi(1020)$, whose masses are pretty close to the K^+K^- threshold. Some experiments of K^+K^- scattering are conducted at the cooler synchrotron COSY facilities [2–7], where the prompt K^+K^- spectrum is expressed by a four-body phase-space distribution altered by various final state interactions, which indicates a strong evidence of K^+K^- background. Silarski et al. first extracted K^+K^- scattering length: $a_{K^+K^-} = [(0.2^{+0.8}_{-0.2}) + i(0.4^{+0.6}_{-0.4})] \text{ fm}$ [6, 7] via the low energy K^+K^- invariant mass distributions and the generalized Dalitz plot analysis [6, 7]. Moreover, Ablikim et al. consider ρ meson decay to K^+K^- if its mass is larger than K^+K^- threshold [8]. A clear signal in the $f'_2(1525)$ region as well as a nonresonant component was observed in the $K\bar{K}$ mass spectrum [9]. A partial wave analysis of the centrally produced K^+K^- system has been carried out to observe the peaks in the s -wave corresponding to the $f_0(1500)$ and $f_0(1710)$, even the d -wave indicating the evidence for the $f_2(1270)/a_2(1320)$, $f'_2(1525)$ and $f_2(2150)$ [10]. The possibility to measure χ_{c0} in the K^+K^- channel are recently reported in [11]. Furthermore, $K\bar{K}$ interactions are very fundamental to many other interesting physics phenomena, e.g., a study of neutron star properties due to possible Bose-Einstein condensation [12] since kaons are bosons, and there was a pioneering lattice study on kaon condensation [13].

Although the study of K^+K^- scattering length from QCD is a non-perturbative problem in essence, some theoretical efforts are still being made to study $K\bar{K}/K^+K^-$ scattering [14–16]. To understand the intrinsic nature of scalar mesons in terms of quark and gluon constituents the K^+K^- couplings of the isoscalar scalar mesons σ and $f_0(980)$ are investigated [17].

Lattice QCD is at present the unique non-perturbative way which allows us to evaluate K^+K^- scattering length from first principles. Nevertheless, so far, no lattice QCD study on it has been reported because it is very difficult to compute vacuum diagram [1]. Motivated by NPLQCD

benchmark work on K^+K^+ scattering [18] and our exploratory work on $K\bar{K}$ scattering in the $I = 1$ channel [1], we further probe K^+K^- scattering from lattice QCD. The computations are launched on a $20^3 \times 48$ MILC full QCD gauge configuration with the $2 + 1$ flavors of the Asqtad improved staggered sea quarks at $m_\pi \approx 240$ Mev and lattice spacing $a \approx 0.15$ fm [19, 20].

Let us learn scattering of two Nambu-Goldstone kaons with zero momentum in the staggered fermion formalism [21–23]. Using operators $\mathcal{O}_{K^+}(x_1)$ and $\mathcal{O}_{K^-}(x_2)$ for K^+ and K^- at points x_1, x_2 , respectively, we write K^+K^- four-point function as

$$C_{K^+K^-}(t_4, t_3, t_2, t_1) = \sum_{\mathbf{x}_1, \mathbf{x}_2} \sum_{\mathbf{x}_3, \mathbf{x}_4} \langle \mathcal{O}_{K^+}(x_4) \mathcal{O}_{K^-}(x_3) \mathcal{O}_{K^+}^\dagger(x_2) \mathcal{O}_{K^-}^\dagger(x_1) \rangle,$$

with the kaon interpolating field operators defined by $\mathcal{O}_{K^+}(x) = \bar{s}(x)\gamma_5 u(x)$ and $\mathcal{O}_{K^-}(t) = \bar{u}(x)\gamma_5 s(x)$, where $x_1 \equiv (\mathbf{x}_1, t_1)$, and likewise for x_2, x_3 and x_4 . In the isospin limit, the diagrams contributing to the four-point function $C_{K^+K^-}$ corresponding to the terms (1)–(4) in Appendix A of Ref. [1] are shown in Fig. 1 of Ref. [1]. To prevent the Fierz rearrangement of quark lines [22, 23], we opt $t_1 = 0, t_2 = 1, t_3 = t$, and $t_4 = t + 1$. In Fig. 1 we illustrated the quark line diagrams, which are labeled as direct (D), rectangular (R_u/R_s), and vacuum (V) diagrams, respectively [1]. The direct diagram can be easily calculated. However, other three diagrams require extra quark propagator connecting time slices t_3 and t_4 [1].

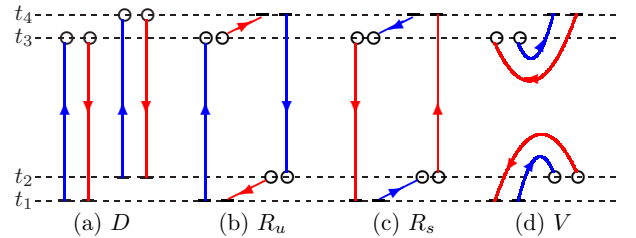


FIG. 1: (color online). Quark-line diagrams contributing to K^+K^- four-point functions. Short bars show wall sources. Open circles are sinks for local K^+/K^- operators. Blue and red lines are u/d and strange quark lines, respectively.

We compute these diagrams by the moving wall sources technique introduced by Kuramashi et al [22, 23]. The concrete lattice calculation of these diagrams are described in Ref. [1]. The rectangular and vacuum diagrams create gauge-variant noise [22, 23], and we usually reduce it by conducting gauge field average without gauge fixing [1, 25–28]. In terms of four diagrams in Fig. 1, K^+K^- correlation function can be expressed as [1],

$$C_{K^+K^-}(t) = D - N_f R_u - N_f R_s + V,$$

where the staggered-flavor factor N_f is inserted to correct for the extra factors N_f in valence fermion loops [21]. The four-fold degeneracy of staggered sea quarks is removed by taking the fourth root of the staggered fermion determinant [21, 29]. The s -wave K^+K^- scattering length in the continuum is defined in terms of phase shift δ_0 by [1] $a_0 = \lim_{k \rightarrow 0} \frac{\tan \delta_0(k)}{k}$, where the scattering is purely elastic below inelastic thresholds. We should remember that the truncation of the effective range r serves as a source of the systematic uncertainty which appears as $\mathcal{O}(1/L^6)$ and hence we ignore it [1]. The scattering momentum k is related to total energy of K^+K^- system by

$$E_{K^+K^-} = 2\sqrt{m_K^2 + k^2}, \quad (1)$$

and $\delta_0(k)$ is evaluated by Lüscher's formula [30],

$$\left(\frac{\tan \delta_0(k)}{k}\right)^{-1} = \frac{\sqrt{4\pi}}{\pi L} \cdot \mathcal{Z}_{00} \left(1, \frac{k^2}{(2\pi/L)^2}\right), \quad (2)$$

here the zeta function \mathcal{Z}_{00} is formally denoted by

$$\mathcal{Z}_{00}(1; q^2) = \frac{1}{\sqrt{4\pi}} \sum_{\mathbf{n} \in \mathbb{Z}^3} \frac{1}{n^2 - q^2}, \quad q = \frac{L}{2\pi} k$$

and can be calculated by the approach described in [31]. The energy $E_{K^+K^-}$ can be obtained from K^+K^- four-point function with large t , whose behavior is given as [32]

$$C_{K^+K^-}(t) = Z_{K^+K^-} \cosh \left[E_{K^+K^-} \left(t - \frac{T}{2} \right) \right] + (-1)^t Z'_{K^+K^-} \cosh \left[E'_{K^+K^-} \left(t - \frac{T}{2} \right) \right] + \dots \quad (3)$$

The oscillating term corresponding to the contributions from the intermediate states with opposite parity is a characteristic of the Kogut-Susskind formulation [32].

In practice, we also calculate the ratios [1]

$$R^X(t) = \frac{C_{K^+K^-}^X(0, 1, t, t+1)}{C_K(0, t)C_K(1, t+1)}, \quad X = D, R_u, R_s \text{ and } V, \quad (4)$$

where C_K is kaon two-point function. We can verify that when $t \ll T/2$, even we impose periodic boundary condition in the temporal direction, we still can roughly extract the energy shift from these ratios.

We should bear in mind that the contributions of non-Nambu-Goldstone kaons in the intermediate states is exponentially suppressed for large time region due to their heavier masses compared to these of Goldstone kaon [21]. Therefore we neglect this systematic error.

In this work we measured K^+K^- four-point function on a MILC lattice ensemble of $601 \cdot 20^3 \times 48$ gauge configurations in the presence of the $2+1$ dynamical flavors of the Asqtad-improved staggered fermions with bare quark masses $am_{u/d}/am_s = 0.00484/0.0484$ and bare gauge coupling $10/g^2 = 6.566$ [19, 20]. The inverse lattice spacing $a^{-1} = 1.373^{+35}_{-13}$ GeV [19, 20]. The strange quark mass is fixed to its physical value [19, 20]. Periodic boundary condition is applied to spatial and temporal directions.

We employ standard conjugate gradient method to compute the required matrix element of inverse fermion matrix. We compute the correlators on each of the 48 time slices, and explicitly combine these results. After averaging the correlator over all 48 possible values, the statistics are greatly improved. For each time slice, six fermion matrix inversions are required corresponding to the possible 3 color choices for each kaon source. Totally we conduct 288 inversions on a single configuration.

In Fig. 2, the individual ratios, R^X ($X = D, R_u, R_s$ and V) are shown as the functions of t . The value of the direct amplitude R^D is pretty close to unity. After an initial increase up to $t \sim 4$, the rectangular R^{R_u} and R^{R_s} amplitudes demonstrates a roughly linear decrease up to $t \sim 18$, and the oscillating behavior in large time region is clearly observed [32]. The features are what we expected [1, 21, 32]. We also notice that R^{R_s} oscillate strongly than R^{R_u} . The physical meaning of the intense oscillation of R^{R_s} and its mass dependence is not clear to us, which are needed to be further investigated.

The vacuum amplitude is pretty small up to $t \sim 8-13$, and loss of signals after that. Since its correlation functions reflect the quantum fluctuations of QCD vacuum, the error for disconnected amplitude should be roughly independent of t [33], thus the error of $R^V(t)$ grows exponentially as $e^{2m_K t}$ [1] for large t . While the analytical arguments in [33] suggests the error of ratio for rectangular R_u diagram grow exponentially as $e^{(2m_K - m_{s\bar{s}})t}$, where $m_{s\bar{s}}$ is a fictitious meson with two valence quarks mass about m_s (likewise for R_s diagram as $e^{(2m_K - m_\pi)t}$)¹. The magnitudes of errors are in quantitative agreement with these predictions as exhibited in Fig. 3. Fitting these errors $\delta R^X(t)$ by a single exponential $\delta R^X(t) \sim e^{\mu_X t}$ for $8 \leq t \leq 18$, we get $a\mu_X = 0.246, 0.581$ and 0.755 for $X = R_u, R_s$ and V , which can be compared with our determinations of $am_\pi = 0.1750(2)$, $am_K = 0.3774(2)$ and $am_{s\bar{s}} = 0.5012(2)$ on the same set of gauge configu-

¹ For the MILC gauge configuration used in [1], we can easily check that $m_\pi \approx 2m_K - m_{s\bar{s}}$ and $m_{s\bar{s}} \approx 2m_K - m_\pi$.

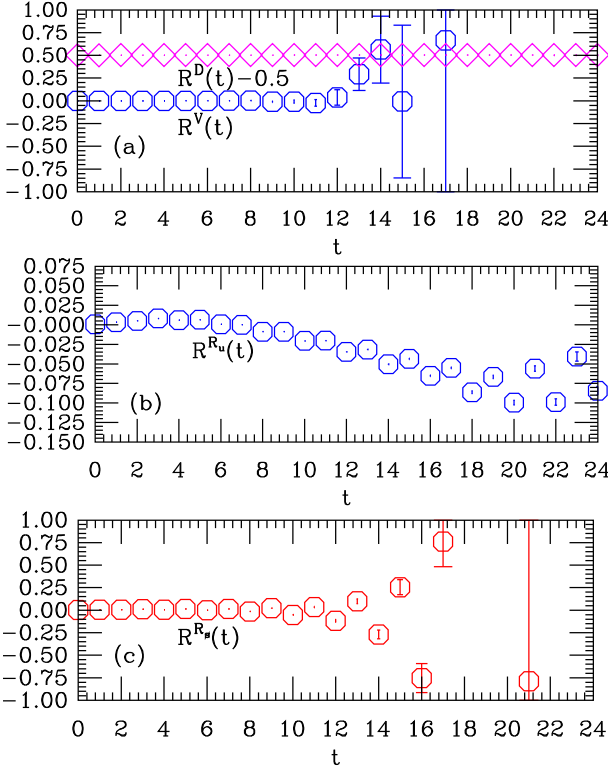


FIG. 2: (color online). Individual ratios $R^X(t)$ ($X = D, R_u, R_s$ and V) for K^+K^- four-point function as functions of t . (a) Direct diagram shifted by 0.5 (red diamonds) and vacuum diagram (blue octagons); (b) Rectangular diagram R_u (blue octagons); (c) Rectangular diagram R_s (red octagons).

rations. In principle, we can reasonably assume that the vacuum amplitude is still small for large t , and ignore it in the following analysis [22]. Nevertheless, we will include it such that the calculation has integrity.

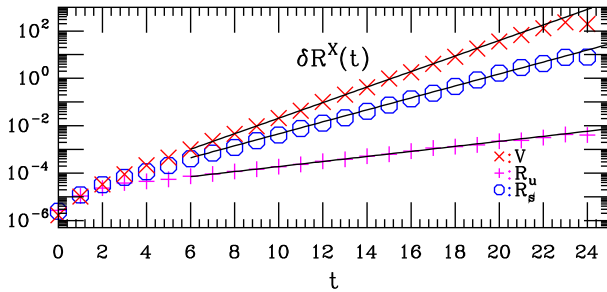


FIG. 3: (color online). Error of ratios $R^X(t)$ ($X = R_u, R_s$ and V) as functions of t . Solid lines are single exponential fits over $8 \leq t \leq 16$.

We use Eq. (3) to extract the energy aE , then insert it into Eq. (2) to obtain the scattering length. In practice, we select the energy aE by looking for a combination of a “plateau” in the energy as a function of the minimum distance D_{\min} and a good confidence level (χ^2/dof) for the fit [1]. The K^+K^- correlation function is plotted in Fig. 4, where we can watch fitted functional form as

compared with lattice data. As we expected, the systematically oscillating feature in the large time region is clearly observed [32]. The scattering momentum k^2 in lattice unit calculated by Eq. (1) and then s -wave scattering length $a_0^{K^+K^-}$ obtained through Eq. (2), together with fitted values of aE , fitting range and fitting quality (χ^2/dof) are listed in Table I. The errors of scattering momentum k and scattering length are calculated from the statistic errors of the energy aE and kaon mass am_K . The errors quoted for $a_0^{K^+K^-}$ are statistical only.

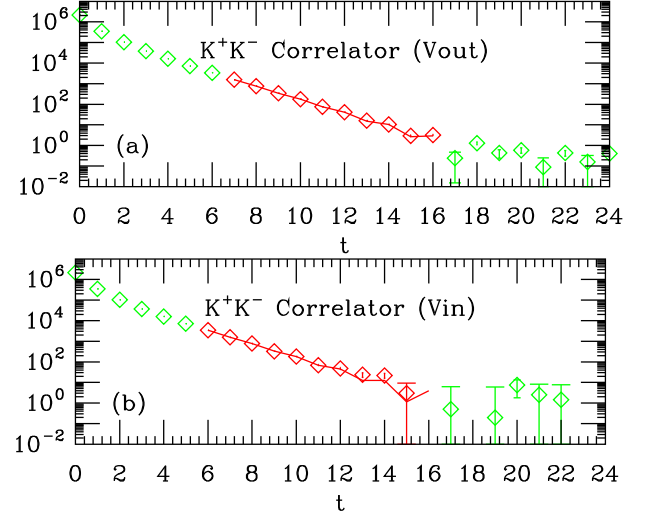


FIG. 4: (color online). The K^+K^- correlation function. The fitting range is indicated by points and fitted lines in red (darker points and lines). (a) The result excluding vacuum diagram. (b) The result including vacuum diagram. Occasional points with negative central values are not plotted.

TABLE I: Summary of the s -wave K^+K^- scattering length. $am_K = 0.3777(2)$ and $af_\pi = 0.1177(4)$ are used to estimate the tree-level prediction value in Eq. (5). The energy E and scattering momentum k are listed in lattice units. Column two show the results left vacuum diagram out. Column three display the results with the inclusion of vacuum diagram. Fitting range and fit quality (χ^2/dof) are listed as well.

	Lat. Results(Vout)	Lat. Results(Vin)	Tree Level
	Fit A	Fit B	
$m_K a_0^{K^+K^-}$	1.122(170)	0.873(520)	0.8188(61)
$E_{K^+K^-}$	0.74698(85)	0.74839(306)	
k^2	-0.00608(62)	-0.00519(216)	
Range	7 – 16	6 – 16	
χ^2/dof	11.5/6	9.0/7	

In Table I we also list the s -wave K^+K^- scattering length predicted by the tree level χ PT formula [1, 14, 15]

$$m_K a_0^{K^+K^-} = \frac{1}{4\pi} \frac{m_K^2}{f_\pi^2}. \quad (5)$$

where we substituted the corresponding kaon mass m_K and the pion decay constant f_π determined on the same

set of gauge configurations. We noted that the simulation results are consistent with Eq. (5) within $1 \sim 2$ standard deviations, which we find pretty satisfactory considering the systematic uncertainties discussed above [1].

It is definitely surprising that the extracted scattering lengths are in reasonable agreement, within uncertainties, with the tree-level prediction of $SU(3)$ χ PT, considering one open question that tree-level χ PT calculation for K^+K^- scattering length are certainly not accurate enough since one has the f_0 and a_0 resonances close by which make the nonperturbative calculation imprecise, maybe one-loop χ PT calculation and potential contributions from higher order effects are probably important. This is somewhat similar to the cleaner case of K^+K^+ scattering length [18] where there are no resonances near by. However, we should keep firmly in mind that there still exist a large statistical error for Fit A (without including vacuum term) and big error in Fit B (including vacuum diagram) as we predicted in [1].

In summary, in this work, we conducted the realistic ab initio lattice QCD calculation of s -wave K^+K^- scattering length, where the rectangular and vacuum diagrams play a crucial role. We employed the technique of the moving wall sources without gauge fixing [22, 23] to calculate all the four diagrams, and observed a clear signal of the attraction. We, first from lattice QCD, obtained its s -wave scattering length $m_K a_0^{K^+K^-} = 0.873(520)$, or $a_0^{K^+K^-} = 0.456 \pm 0.272$ fm, which is in fair agreement with the tree level χ PT predictions [1, 14, 15].

Moreover, M. Silarski et al. carried out a special fit for us and achieved the experimental value of the s -wave K^+K^- scattering length: $a_0^{K^+K^-} = 3.5_{-2.0}^{+3.0}$ fm [34], which was obtained by setting the imaginary part of K^+K^- scattering length to be zero when fitting their experimental data [6, 7]. But due to the low statistics, the uncertainties are still rather large. It is quite encouraging that with the current computing resources, we still can compute the K^+K^- scattering length and which can be comparable with the above experimental value.

Since this is a first lattice QCD evaluation of K^+K^- scattering length, our primary goal is to show the approach in a conceptually clean way. Checks for systematic errors including the discretization error, finite volume effect, and so on, are being investigated on larger MILC lattice ensembles: $24^3 \times 64$ and $28^3 \times 96$, even $48^3 \times 144$. Moreover, it will be important to repeat this calculation using more MILC lattice ensembles such that a continuum extrapolation can be performed. Furthermore, the study of K^+K^- scattering in the multi-channel scattering (e.g., $\pi\pi$ and $K\bar{K}$ two channels) [35] is under preparation, where we will explicitly consider the a_0/f_0 resonance [36]. We anticipate that these sophisticated lattice computations of strong K^+K^- scattering length would be a specially important source for further progress toward a better understanding of some reactions like $pp \rightarrow ppK^+K^-$, and so on.

The author appreciates the MILC Collaboration and NERSC for supplying us the Asqtad lattice ensemble. We specially thank Silarski and his colleagues for their conducting a special fit to compare with lattice result. The author sincerely thanks Eulogio Oset and Liu Chuan for their valuable comments and Carleton DeTar for providing us the fitting software. We deeply thanks Paul Kienzle for his teaching us many computation skills for this work during my work in NIST, Gaithersburg, USA. The author thankfully acknowledge the computer resources and technical support provided by the Institute of Nuclear Science and Technology, Sichuan University (specially Hou Qing, Zhu An and Ning Liu).

-
- [1] Z. Fu, Eur. Phys. J. C (2012) **72**, 2159 (2012).
 - [2] P. Winter *et al.*, Phys. Lett. **B 635**, 23 (2006).
 - [3] A. Dzyuba *et al.*, Phys. Lett. **B 668**, 315 (2008).
 - [4] Y. Maeda *et al.*, Phys. Rev. **C 79**, 018201 (2009).
 - [5] J. J. Xie and C. Wilkin, Phys. Rev. **C 82**, 025210 (2010).
 - [6] M. Silarski *et al.*, Phys. Rev. **C 80**, 045202 (2009).
 - [7] M. Silarski, Int. J. Mod. Phys. **A 26**, 539 (2011).
 - [8] M. Ablikim *et al.*, arXiv:1208.2320.
 - [9] R. Aaij *et al.*, Phys. Rev. Lett. **108**, 151801 (2012).
 - [10] D. Barberis *et al.*, Phys. Lett. **B 453**, 305 (1999).
 - [11] P. Lebiedowicz and A. Szczurek, Phys. Rev. **D 85** (2012) 014026.
 - [12] G. -Q. Li, C. H. Lee and G. E. Brown, Nucl. Phys. **A 625**, 372 (1997).
 - [13] W. Detmold, K. Orginos, M. J. Savage and A. Walker-Loud, Phys. Rev. **D 78**, 054514 (2008).
 - [14] J. A. Oller, E. Oset and J. R. Pelaez, Phys. Rev. **D 59**, 074001 (1999).
 - [15] F. Guerrero and J. A. Oller, Nucl. Phys. **B 537**, 459 (1999).
 - [16] Z.H. Guo and J.A. Oller, Phys. Rev. **D 84**, 034005 (2011).
 - [17] R. Kaminski, G. Mennessier and S. Narison, Phys. Lett. **B 680**, 148 (2009).
 - [18] S. R. Beane *et al.*, Phys. Rev. **D 77**, 094507 (2008).
 - [19] C. Bernard *et al.*, Phys. Rev. **D 83**, 034503 (2011).
 - [20] A. Bazavov *et al.*, Rev. Mod. Phys. **82**, 1349 (2010).
 - [21] S. R. Sharpe, R. Gupta and G. W. Kilcup Nucl. Phys. **B 383**, 309 (1992).
 - [22] Y. Kuramashi *et al.*, Phys. Rev. Lett. **71** (1993) 2387.
 - [23] M. Fukugita *et al.*, Phys. Rev. **D 52**, 3003 (1995).
 - [24] Z. Fu, Phys. Rev. **D 85**, 074501 (2012).
 - [25] Z. Fu, J. High Energy Phys. **01** (2012) 017.
 - [26] Z. Fu, J. High Energy Phys **07** (2012) 142.
 - [27] Z. Fu, Commun. Theor. Phys. **57**, 78 (2012).
 - [28] Z. Fu and K. Fu, Accepted 10/15/12 by: Phys. Rev. **D**, arXiv:1209.0350 [hep-lat].
 - [29] T. DeGrand and C. E. Detar, New Jersey, USA: World Scientific (2006) 345 p.
 - [30] M. Luscher, Nucl. Phys. **B 354**, 531 (1991).
 - [31] T. Yamazaki *et al.* Phys. Rev. **D 70**, 074513 (2004).
 - [32] A. Mihaly *et al.*, Phys. Rev. **D 55**, 3077 (1997).
 - [33] G. P. Lepage, CLNS-89-971.
 - [34] Private communication, M. Silarski (2012).
 - [35] S. He, X. Feng and C. Liu, JHEP **0507**, 011 (2005).
 - [36] C. Hanhart, Phys. Lett. **B 715**, 170 (2012).